

Complete spectroscopy of  $^{30}\text{P}$ C. A. Grossmann,<sup>1,2,\*</sup> M. A. LaBonte,<sup>1,2,†</sup> G. E. Mitchell,<sup>1,2</sup> J. D. Shriner,<sup>1,2,‡</sup> J. F. Shriner, Jr.,<sup>3</sup>  
G. A. Vavrina,<sup>1,2,§</sup> and P. M. Wallace<sup>2,4,\*\*</sup><sup>1</sup>North Carolina State University, Raleigh, North Carolina 27695-8202<sup>2</sup>Triangle Universities Nuclear Laboratory, Durham, North Carolina 27708-0308<sup>3</sup>Tennessee Technological University, Cookeville, Tennessee 38505<sup>4</sup>Duke University, Durham, North Carolina 27708-0305

(Received 21 March 2000; published 25 July 2000)

The  $^{29}\text{Si}(p, \gamma)^{30}\text{P}$  reaction was studied for 32 resonances in the energy range  $E_p = 1.0\text{--}2.5$  MeV. Angular distributions were measured for 230 primary and secondary transitions. Results from the analysis of these data were combined with previous measurements of the  $^{29}\text{Si}(p, p_0)^{29}\text{Si}$  and  $^{29}\text{Si}(p, \gamma)^{30}\text{P}$  reactions to determine the spin  $J$ , parity  $\pi$ , and isospin  $T$  of many levels. Remaining ambiguities were eliminated by comparison with the spectrum of the parent nucleus  $^{30}\text{Si}$  and with the calculated shell-model spectrum.  $J$ ,  $\pi$ , and  $T$  have been assigned for 103 states up to an excitation energy of 8.0 MeV.

PACS number(s): 27.30.+t, 21.10.Hw, 25.40.Lw, 25.40.Ny

## I. INTRODUCTION

Following its introduction by Wigner [1], random matrix theory (RMT) [2] was primarily used in the description of compound nuclear states. Recently there has been an explosion of applications of RMT in a wide variety of fields: the recent review by Guhr, Müller-Groeling, and Weidenmüller [3] lists over 800 references. In nuclear physics, analysis of high quality neutron and proton resonance data from a variety of nuclides led to excellent agreement with the relevant version of RMT—the Gaussian orthogonal ensemble (GOE) [4–6]. Following the suggestion by Bohigas *et al.* [7] that quantum systems whose classical analogs were chaotic would show eigenvalue fluctuations that agree with GOE, level statistics have been widely used as “signatures of chaos.”

In spite of the fact that RMT originated in nuclear physics, there have been few experimental tests of RMT in the nucleus. The reason is simple—the standard measures employed to analyze the eigenvalue distribution are extremely sensitive. The spectrum must be pure (no misassigned quantum numbers) and complete (no missing levels). There are very few data sets that satisfy these stringent criteria. The only direct way to test RMT in nuclei is to measure all of the states in a region and determine all of their quantum numbers. In other words, one requires complete spectroscopy.

One would like to examine the statistical properties in different energy regions: near the ground state, in the resonance region, and at energies between these two regimes. Ideally this information should be in a single nuclide. If one adds the requirement that the number of states is reasonably large, say of order 100, then complete spectroscopy is avail-

able for only one nuclide— $^{26}\text{Al}$  [8,9]. Analysis of the energy eigenvalues in  $^{26}\text{Al}$  showed behavior between GOE and Poisson [10,11].

In addition to providing a complete spectrum from the ground state to about 8 MeV excitation energy, the nuclide  $^{26}\text{Al}$  has the special feature that the  $T=0$  and 1 states coexist from the ground state. Although statistical limitations precluded a definitive conclusion, these data provided an experimental test of the effect of symmetry breaking on level statistics. The data were consistent with the general prediction [12,13] that even a small symmetry breaking (isospin symmetry is broken by about 3% in  $^{26}\text{Al}$ ) can have a large effect. A detailed theoretical study by Guhr and Weidenmüller [14] analyzed the effect of breaking isospin symmetry on the eigenvalue distribution. Although there have been no other experimental tests in a quantum system, there have been tests in analog systems—acoustic resonances in quartz blocks [15] and electromagnetic resonances in superconducting microwave billiards [16]. In the former case the symmetry breaking was simulated by removing an octant of a sphere from one corner of the block. In the latter experiment two coupled billiards were employed and the symmetry breaking was simulated by changing the strength of the coupling. In both cases the results were consistent with theoretical predictions and with our original experiment.

RMT also makes an explicit prediction for the distribution of transition matrix elements—the amplitudes should be Gaussian distributed. As a consequence the distribution of the strengths (the amplitudes squared) is a  $\chi^2$  of one degree of freedom—the Porter-Thomas (PT) distribution. There are numerous experimental data sets that agree with the PT distribution. However, theoretical studies concerning transition strength distributions are much more limited than those for eigenvalue distributions. Until very recently there was no theoretical prediction of the effect of symmetry breaking on the transition distribution. Our analysis of the  $^{26}\text{Al}$  transition data [17] indicated that the strength distributions deviate appreciably from the Porter-Thomas distribution. Preliminary theoretical results [18,19] suggest that symmetry breaking does change the transition strength distribution from the

\*Present address: Avant! Corporation, Durham, NC 27703.

†Present address: U.S. Navy, Norfolk, VA 23513.

‡Present address: Upperman High School, Baxter, TN 38544.

§Present address: Landstuhl Regional Medical Center, D-09180 Landstuhl, Germany.

\*\*Present address: Berry College, Mount Berry, GA 30149.

Porter-Thomas distribution, in qualitative agreement with our experimental results. There have been no corresponding measurements with analog systems.

Since the effect of symmetry breaking on statistical distributions has been studied only for  $^{26}\text{Al}$ , complete spectroscopy for another nuclide would be very interesting. We chose  $^{30}\text{P}$  as our candidate for study because it is similar to  $^{26}\text{Al}$  in many respects: it is an  $N=Z$  odd-odd nuclide, the two isospins coexist from the ground state, and the level density is comparable to that in  $^{26}\text{Al}$ .

Previous measurements on  $^{30}\text{P}$  are summarized in the most recent data compilation [20]. The key reactions for our spectroscopic studies are the  $(p,p)$  and  $(p,\gamma)$  reactions. Our group [21] had performed a high resolution study of the  $^{29}\text{Si}(p,p_0)$  and  $^{29}\text{Si}(p,p_1)$  reactions and identified 66 resonances in the energy range  $E_p = 1.29 - 3.30$  MeV. We then performed another high resolution study [22] of the  $^{29}\text{Si}(p,\gamma)$ ,  $^{29}\text{Si}(p,p_1\gamma)$ , and  $^{29}\text{Si}(p,p_2\gamma)$  reactions, primarily to identify weak resonances. Earlier measurements of the  $(p,\gamma)$  reaction on  $^{29}\text{Si}$  had been performed by Reinecke *et al.* [23] and by Cameron [24]. Because of the need for completeness and purity, we remeasured the  $^{29}\text{Si}(p,\gamma)$  reaction with our very good beam energy resolution and good detector resolution. These results were reported by Wallace *et al.* [25] and Vavrina *et al.* [26].

At this stage we had observed nearly every state in  $^{30}\text{P}$  up to 8.0 MeV, knew the spins and parities for the majority of the states (and had placed limitations on the possible assignments for most of the remaining states), and had information on the isospin of many states. However, a large number of uncertainties for the quantum number assignments remained. We report here the results from  $^{29}\text{Si}(p,\gamma)$  angular distribution measurements for many of the resonances. With this additional information, we either have definite spin and parity assignments or have placed stringent limitations on the spin-parity possibilities for almost every level. We have identified essentially every  $T=1$  state as the analog of a state in the parent nucleus  $^{30}\text{Si}$  and essentially every positive parity state with the levels predicted by a shell-model calculation [27]. In this paper we present the experimental results and provide our final quantum number assignments for the states in  $^{30}\text{P}$ . In a subsequent paper we will present an analysis of the eigenvalue distributions and the transition strength distributions.

In Sec. II we present the relevant angular distribution formalism. In Sec. III the experimental setup is described. The method of analysis and an example are given in Sec. IV. The quantum number assignments are presented in Sec. V. Section VI is a brief summary.

## II. ANGULAR DISTRIBUTIONS

### A. General

We use the standard density-efficiency matrix approach to describe the reaction and follow the formulation by Ferguson [28]. We assume compound nucleus formation and isolated resonances. The target spin  $A$  couples to projectile spin  $i$  to form channel spin  $s$ . The channel spin is coupled with the relative orbital angular momentum  $l$  of the target and projec-

tile to form a compound state with total angular momentum  $J$ . These spin couplings are given by  $\vec{A} + \vec{i} = \vec{s}$  and  $\vec{s} + \vec{l} = \vec{J}$ . Parity conservation requires that  $\pi_J = \pi_A \pi_i (-1)^l$ .

A primary transition is a  $\gamma$ -ray transition from the compound state to a residual state. In the exit channel, the residual state angular momentum  $C$  and the  $\gamma$ -ray multipolarity  $L$  couple to the compound state angular momentum  $J$ , given by  $\vec{C} + \vec{L} = \vec{J}$ . The angular distribution for this reaction can be written [28] as

$$\begin{aligned} \frac{d\sigma}{d\Omega} \propto & \left( \frac{\lambda}{i\hat{A}} \right)^2 \sum (-1)^{(s-l_1+l_2-2J_2+C-L_1+L_2)} \\ & \times \bar{Z}(l_1 J_1 l_2 J_2; s k) \bar{Z}_1(L_1 J_1 L_2 J_2; C k) \langle J_1 || l_1 s \rangle \\ & \times \langle J_2 || l_2 s \rangle^* \langle CL_1 || J_1 \rangle \langle CL_2 || J_2 \rangle^* Q_k P_k(\cos \theta), \end{aligned} \quad (1)$$

with the summation over  $l_1$ ,  $l_2$ ,  $L_1$ ,  $L_2$ ,  $J_1$ ,  $J_2$ ,  $s$ , and  $k$ . The  $\bar{Z}$  coefficient is given by Huby [29] as a modification to the  $Z$  coefficient of Blatt and Biedenharn [30]. The  $\bar{Z}_1$  coefficient is discussed by Biedenharn [31].  $Q_k$  is the correction factor due to the finite detector size,  $\theta$  is the angle between the beam and detector, and  $P_k$  is the Legendre polynomial of order  $k$  ( $k$  satisfies the relations  $\vec{k} = \vec{l}_1 + \vec{l}_2$ ,  $\vec{k} = \vec{L}_1 + \vec{L}_2$ , and  $\vec{k} = \vec{J}_1 + \vec{J}_2$ ). The notation used for the reduced matrix elements [32] distinguishes between emission and absorption matrix elements. The final spins are written on the left-hand side of the matrix element and the initial spins on the right. The initial and final spins are separated by a double vertical bar.

Biedenharn [31] showed that in the single-level approximation the scattering matrix element can be expressed as

$$\langle J || l s \rangle \langle CL || J \rangle \approx \frac{e^{i\xi_l} g_s l g_L}{E_r - E - \frac{i\Gamma}{2}}. \quad (2)$$

Here  $g_c$  is the square root of the partial width of the resonance in channel  $c$ ,  $E_r$  is the resonance energy,  $\Gamma$  is the total width of the resonance, and  $\xi_l$  is an energy-dependent phase shift. The phase shift includes both Coulomb and hard sphere scattering and depends on kinematic parameters;  $\xi_l$  was evaluated for each resonance.

### B. $^{29}\text{Si}$

Since the proton has  $i = \frac{1}{2}$  and the  $^{29}\text{Si}$  target nucleus  $A = \frac{1}{2}$ , the channel spin is  $s = 0$  or  $1$ . The compound and residual states ( $J$  and  $C$ ) are states of  $^{30}\text{P}$ . Since the resonances studied in this experiment are well isolated,  $J_1 = J_2 \equiv J$ . With only integral values allowed for both  $s$  and  $l$ ,  $J$  must also be an integer. Since the parities of the proton and the target are the same,  $l$  has the same parity as the compound state:  $\pi_J = (-1)^l$ . Therefore if there is any  $l$  mixing, the two values of  $l$  must have the same parity. The compound nuclear state  $J$  decays to a final state  $C$ , and the two states may have the same or different parities. When the

parities are the same (different), the parity of the radiation must be even (odd). The parity of the radiation is  $\pi(ML) = (-1)^{L+1}$  or  $\pi(EL) = (-1)^L$ . We consider only  $E1$ ,  $E2$ ,  $E3$ ,  $M1$ , and  $M2$  multipoles, and mixing of at most two multipoles.

At these low energies, we assume that  $l \leq 4$  and therefore  $J \leq 5$  for the compound nuclear states. Because of the Clebsch-Gordon coefficient [contained in the  $\bar{Z}(l_1 J l_2 J; sk)$  term] and the fact that parity is conserved,  $k$  is even. The  $Q_k$  terms are calculated for each transition using Monte Carlo methods [33]. Equation (1) can be rewritten

$$\begin{aligned} \frac{d\sigma}{d\Omega} &= \sum_{k=0,2,4,6} A_k Q_k P_k(\cos \theta) \\ &= A_0 \left[ 1 + \sum_{k=2,4,6} a_k Q_k P_k(\cos \theta) \right], \end{aligned} \quad (3)$$

where  $a_k \equiv A_k/A_0$ ,  $A_0$  is an overall normalization factor,  $Q_0 \equiv 1$ , and  $P_0 \equiv 1$ .

The  $a_k$ 's are expressed most simply in terms of ratios of the  $g$ 's, the square roots of the resonance partial widths. Mixing ratios are defined as the square root of the ratio of resonance partial widths in two channels. For  $A = 1/2$  there is proton entrance channel mixing for either  $s$  or for  $l$ , but not both simultaneously. The proton mixing ratio is defined with the lower value of  $s$  or  $l$  in the denominator; for example, the mixing ratio of  $\{s=1, l=3\}$  and  $\{s=1, l=1\}$  channels is  $\delta_p \equiv g_{13}/g_{11}$ . Similarly,  $\gamma$ -ray mixing ratios are defined with the lower value of  $L$  in the denominator, consistent with the phase convention of Rose and Brink [34]. We assume that significant mixing in the  $\gamma$ -ray channel occurs only between  $M(L)$  and  $E(L+1)$  channels. The  $\gamma$ -ray mixing ratio is therefore defined as  $\delta_\gamma \equiv (g_{E(L+1)}/g_{M(L)})$ . Since multipolarities higher than  $E3$  are not considered,  $L \leq 3$  and  $k \leq 6$ .

### C. Example

Consider a transition from a  $J^\pi = 2^+$  compound state to a  $C^\pi = 1^+$  residual state. Since  $J$  has even parity,  $l$  must be even. Both  $s$  values allow only  $l=2$ . The allowed  $L$  values range from 1 to 3. Since the parities of  $J$  and  $C$  are the same, the electromagnetic character  $QL$  can be  $M1$  or  $E2$ . For a maximum  $L$  value of 2, the maximum  $k$  value is 4.

For these  $(s, l)$  and  $QL$  combinations the mixing ratios are  $\delta_p = g_{12}/g_{02}$  and  $\delta_\gamma = g_{E2}/g_{M1}$ . The phase shifts  $\xi_i$  cancel when  $a_2$  and  $a_4$  are formed. The coefficients for this transition are

$$a_2 = -\frac{1}{28} \frac{(2 + \delta_p^2)(7 + 14\sqrt{5}\delta_\gamma - 5\delta_\gamma^2)}{(1 + \delta_p^2)(1 + \delta_\gamma^2)} \quad (4)$$

and

$$a_4 = \frac{8}{21} \frac{(3 - 2\delta_p^2)\delta_\gamma^2}{(1 + \delta_p^2)(1 + \delta_\gamma^2)}. \quad (5)$$

### D. Secondary transitions

Secondary transitions ( $\gamma$ -ray transitions originating from a state populated by a primary transition) are treated in a similar way to primary transitions. For secondary transitions the residual state  $C$  emits a secondary  $\gamma$  ray of multipolarity  $L'$  and leaves a final state  $D$ . The coupling is  $\vec{C} = \vec{D} + \vec{L}'$ . The extension of the formalism is straightforward and will not be discussed here. We measured the angular distributions of a large number of secondary transitions and included all of them in our analysis.

## III. EXPERIMENTAL SETUP AND PROCEDURE

It is important that the reaction be studied with both very good beam-energy resolution and good  $\gamma$ -ray energy resolution. The good beam-energy resolution is needed to resolve close-lying resonance states. This resolution was achieved with the KN Van de Graaff accelerator and associated feedback systems of the Triangle Universities Nuclear Laboratory (TUNL) High Resolution Laboratory (HRL) [35]. This system provides overall beam-energy resolution of  $\approx 220$  eV with thin solid targets.

The detector resolution is needed to resolve the large number of  $\gamma$  rays observed at each resonance. The primary  $\gamma$ -ray detection system consisted of a pair of 60% efficient HPGe detectors, one of which was surrounded by a large bismuth germanate (BGO) Compton-suppression shield [36]. The resolution of these detectors was 1.8–2.0 keV full width at half maximum (FWHM) at the 1332-keV  $\gamma$  ray in  $^{60}\text{Co}$ . A silicon surface-barrier detector was located at  $165^\circ$  to detect charged particles, and a  $7.62 \times 7.62$  cm NaI(Tl) detector was placed at  $140^\circ$ . These two detectors were used to measure excitation functions to locate the resonances of interest.

All of the resonances studied in this work had been observed previously in the capture reaction and almost all of them in elastic scattering. For most of the resonances, detailed  $\gamma$ -ray spectra had also been measured [25,26]. In the present measurement the suppressed detector was located at  $90^\circ$  and used for monitoring purposes. The unsuppressed Ge detector was rotated to five different angles:  $25^\circ$ ,  $38^\circ$ ,  $50^\circ$ ,  $63^\circ$ , and  $90^\circ$ . A sample Compton-suppressed spectrum is shown in Fig. 1.

The targets were thin films of Si targets (enriched to 95%  $^{29}\text{Si}$ ) evaporated onto  $5.0 \mu\text{g}/\text{cm}^2$  carbon foils. The targets were either  $1.5$  or  $3.0 \mu\text{g}/\text{cm}^2$  Si, corresponding to a proton energy loss of about 170 or 340 eV for these energies. The thinner targets were used to study narrow resonances or those with close neighbors. These targets were very stable; typical proton beam currents were 6–8  $\mu\text{A}$ .

The resonances that were selected for study either had unknown or ambiguous  $J^\pi$  values or decayed to states that had unknown or ambiguous  $J^\pi$  values. In addition, some resonances were selected for study when the determination of a  $\gamma$ -ray mixing ratio might aid in the isospin assignment for either the resonance or the final state.

The first step was to locate the resonance. Although under favorable conditions the beam energy drift is only about 6 eV/h [37], some resonances were studied for as long as

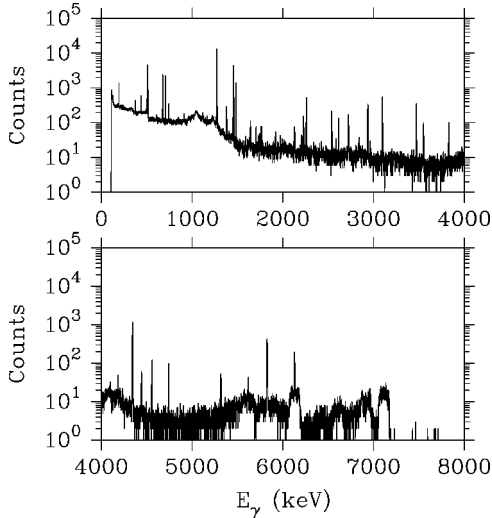


FIG. 1. Compton-suppressed detector spectrum for the  $^{29}\text{Si}(p, \gamma)$  reaction. This spectrum was measured at  $E_p = 1.7450$  MeV.

three days. Therefore we periodically checked to ensure that we were still on resonance. Spectra were recorded (typically for 50 mC integrated beam current at a time) for each of the two detectors at each of the five angles. The entire process was then repeated a number of times to provide adequate statistics—up to 300 mC were accumulated at each angle for the weakest resonances.

The yields of the  $\gamma$  rays of interest were determined from the spectra. (Calibration details are provided by Vavrina *et al.* [26].) Several corrections were applied to the raw data. First a dead time correction was applied. Then the fixed HPGe detector was used as a monitor to account for fluctuations due to changes in target thickness, beam optics, etc. In addition a correction was needed for imperfect geometry—the location where the beam intersects the target is not the exact center of the axis of rotation of the germanium detector. The correction was determined by placing an isotropic source ( $^{152}\text{Eu}$ ) on the target rod of the target chamber and collecting data with the two HPGe detectors at all five angles.

The corrected angular distributions for each transition of interest were then fit to an expansion in Legendre polynomials. A typical angular distribution and fit are shown in Fig. 2. Coefficients were determined for 156 primary and 74 secondary transitions; to conserve space the values are not listed but are available from the authors.

#### IV. RESULTS AND ANALYSIS

Information from the angular distributions is used to place restrictions on the quantum numbers  $J$ ,  $\pi$ , and  $T$ . One key approach compares the strength of the partial  $\gamma$ -ray width in channel  $QL$  for a particular transition with measured transition strengths in this mass region. To make this comparison one needs the total  $\gamma$ -ray width of the initial level  $\Gamma_\gamma$ , as well as the branching ratio  $B_{\gamma,i}$  and multipole mixing ratio

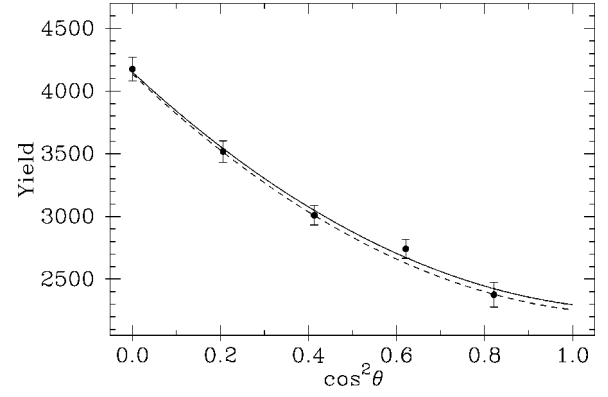


FIG. 2. Fit to the experimental angular distribution for the  $E_x = 7282.0$  keV to  $E_x = 4182.81$  keV transition in  $^{30}\text{P}$ . The solid line shows the best fit using Eq. (3), while the dashed line shows the fit using the extracted mixing ratios.

$\delta_{\gamma,i}$  for a given transition. The partial  $\gamma$ -ray width is the product of the total  $\gamma$ -ray width and the branching ratio, and is also the sum of the  $E(L+1)$  and  $M(L)$  widths. For a particular partial  $\gamma$ -ray width  $i$ , this relation can be written in terms of the mixing ratios as

$$\Gamma_\gamma B_{\gamma,i} = \Gamma_{E(L+1),i} \left( \frac{1}{\delta_{\gamma,i}^2} + 1 \right) = \Gamma_{ML,i} (1 + \delta_{\gamma,i}^2). \quad (6)$$

We first consider these factors, then discuss the recommended upper limits for transition strengths, and finally illustrate with an application of the method.

##### A. Mixing ratios and branching ratios

For the resonance states the measured branching ratios are listed in previous publications [25,26]. For the bound states and for states just above the proton separation energy, the branching ratios obtained in our measurements are listed in Table I.

In order to determine the mixing ratios we wrote a FORTRAN computer program called MIXCALC. The input for this program includes the normalized yields and angles for each transition. The program fits all mixing ratios, both the proton ratio and each of the  $\gamma$ -ray ratios, by performing a simultaneous fit to all primary and secondary angular distributions. The entire calculation is repeated for each set of possible  $J^\pi$  values for both initial and final states.

The analysis is performed sequentially. First we consider only the primary transitions (and the proton entrance channel) and perform a grid search (typically 13 to 19 values per mixing ratio) over the entire range of possible mixing ratios ( $-\infty$  to  $+\infty$ ). For  $M$   $\gamma$ -ray mixing ratios (plus the proton entrance channel) and  $N$  grid points this is  $(M+1)^N$  calculations. A  $\chi^2$  value is obtained by comparing the calculated yields for each set of mixing ratios and experimental  $A_0$  values with the normalized experimental yields. This procedure identifies local minima in the  $\chi^2$  space. In the second

TABLE I.  $\gamma$ -ray branching ratios  $B_\gamma$  from this work for states with  $E_x < 6500$  keV in  $^{30}\text{P}$ . The numbers in parentheses indicate the error on the last digit of the branching ratio. The number to the right of the arrow is the excitation energy of the final state.

$E_i$ (keV)	$B_\gamma$ (%)
1454.2	95.2(8) $\rightarrow$ 0, 4.76(8) $\rightarrow$ 708.7
1973.3	41.5(5) $\rightarrow$ 0, 58.5(7) $\rightarrow$ 708.7
2539.0	96(1) $\rightarrow$ 0, 3.1(1) $\rightarrow$ 708.7, 0.76(5) $\rightarrow$ 1973.3
2723.7	97.5(9) $\rightarrow$ 0, 2.5(2) $\rightarrow$ 708.7
2839.3	22.7(5) $\rightarrow$ 0, 52.1(8) $\rightarrow$ 708.7, 25.3(5) $\rightarrow$ 1454.2
2937.5	17.8(2) $\rightarrow$ 0, 32.4(4) $\rightarrow$ 677.0, 5.40(9) $\rightarrow$ 708.7, 44.0(5) $\rightarrow$ 1454.2, 0.33(3) $\rightarrow$ 1973.3
3019.2	100 $\rightarrow$ 677.0
3733.8	50(1) $\rightarrow$ 0, 32(1) $\rightarrow$ 677.0, 9.8(6) $\rightarrow$ 1454.2, 7.5(5) $\rightarrow$ 2937.5
3835.8	19.2(6) $\rightarrow$ 708.7, 10.0(4) $\rightarrow$ 1454.2, 71(1) $\rightarrow$ 2937.5
3928.6	30(1) $\rightarrow$ 1454.2, 70(1) $\rightarrow$ 2937.5
4143.6	87.0(9) $\rightarrow$ 0, 4.1(3) $\rightarrow$ 708.7, 7.5(4) $\rightarrow$ 1454.2, 1.3(1) $\rightarrow$ 2937.5
4182.8	10.5(3) $\rightarrow$ 0, 1.2(2) $\rightarrow$ 677.0, 76.1(9) $\rightarrow$ 708.7, 2.5(3) $\rightarrow$ 1454.2, 3.5(2) $\rightarrow$ 1973.3, 6.3(3) $\rightarrow$ 2539.0
4232.0	73(1) $\rightarrow$ 1973.3, 24.1(7) $\rightarrow$ 2539.0, 2.6(1) $\rightarrow$ 2839.3
4298.6	100 $\rightarrow$ 1454.2
4343.8	95(2) $\rightarrow$ 1973.3, 5.0(4) $\rightarrow$ 2539.0
4422.8	96(1) $\rightarrow$ 0, 4.1(2) $\rightarrow$ 708.7
4469.1	94(2) $\rightarrow$ 0, 6.1(8) $\rightarrow$ 708.7
4502.2	40(1) $\rightarrow$ 0, 3.5(3) $\rightarrow$ 708.7, 56(1) $\rightarrow$ 1454.2
4625.9	56(1) $\rightarrow$ 1454.2, 15.0(5) $\rightarrow$ 1973.3, 29.3(8) $\rightarrow$ 2937.5
4736.0	11.9(5) $\rightarrow$ 0, 7.5(4) $\rightarrow$ 708.7, 12.2(5) $\rightarrow$ 1454.2, 66(1) $\rightarrow$ 2937.5, 1.9(2) $\rightarrow$ 3019.2
4925.5	10.4(5) $\rightarrow$ 1454.2, 90(3) $\rightarrow$ 4232.0
4937.3	82(3) $\rightarrow$ 677.0, 18(1) $\rightarrow$ 2937.5
4941.4	91(4) $\rightarrow$ 677.0, 9.3(6) $\rightarrow$ 1973.3
5206.8	76(2) $\rightarrow$ 0, 24(1) $\rightarrow$ 708.7
5230.1	50(4) $\rightarrow$ 1973.3, 24(2) $\rightarrow$ 2539.0, 26(2) $\rightarrow$ 2839.3
5411.1	28(6) $\rightarrow$ 1973.3, 41(6) $\rightarrow$ 2839.3, 31(7) $\rightarrow$ 2937.5
5506.4	1.6(3) $\rightarrow$ 0, 96(3) $\rightarrow$ 677.0, 2.4(2) $\rightarrow$ 2937.5
5508.6	52(1) $\rightarrow$ 1454.2, 48(1) $\rightarrow$ 1973.3
5576.3	18(1) $\rightarrow$ 0, 63(2) $\rightarrow$ 708.7, 15(1) $\rightarrow$ 1454.2, 2.0(4) $\rightarrow$ 3733.8, 2.2(3) $\rightarrow$ 3835.8
5701.3	7.0(7) $\rightarrow$ 2539.0, 4.7(6) $\rightarrow$ 2723.7, 75(4) $\rightarrow$ 2937.5, 13.3(9) $\rightarrow$ 4182.8
5934.0	31(1) $\rightarrow$ 1973.3, 2.1(4) $\rightarrow$ 2539.0, 11.9(7) $\rightarrow$ 2839.3, 12.7(7) $\rightarrow$ 2937.5, 42(1) $\rightarrow$ 4343.8
6006.0	32(2) $\rightarrow$ 1454.2, 35(2) $\rightarrow$ 1972.3, 9(1) $\rightarrow$ 2539.0, 14(1) $\rightarrow$ 2723.7, 10(1) $\rightarrow$ 2839.3
6093.5	1.5(4) $\rightarrow$ 2723.7, 2.8(4) $\rightarrow$ 2937.5, 10.6(7) $\rightarrow$ 4143.6, 35(1) $\rightarrow$ 4232.0, 50(2) $\rightarrow$ 4625.9
6229.0	18(3) $\rightarrow$ 1973.3, 7(2) $\rightarrow$ 2539.0, 64(5) $\rightarrow$ 3928.6, 11(2) $\rightarrow$ 4298.6

step these mixing-ratio values are used as starting points for a more detailed search. A  $\chi^2$  minimization procedure is used to explore the local region in the parameter space and to find the best possible local solutions. Since there are often several initial starting points for the detailed search, there are often multiple local solutions. Only those solutions within 1.0 of the best  $\chi^2$  value are retained.

These solutions are then used as starting points to repeat the entire process on the secondary transition mixing ratios. For the first step in this latter search, the values for the mixing ratios for the primary transitions are held fixed. After the grid search for the secondary transition mixing ratios is completed, a final minimization procedure is followed, with all mixing ratios and  $A_0$ 's varied to obtain the best solution. The mixing ratios obtained by this procedure are listed in Table II

for the primary transitions and in Table III for the secondary transitions.

### B. RUL's

Endt [38] tabulated experimental values of  $\gamma$ -ray strengths and classified them by mass region, electromagnetic radiation type  $QL$ , and as isoscalar or isovector (IS or IV). For this  $T_z=0$  nuclide, transitions with  $T_i-T_f=0$  are isoscalar and those with  $|T_i-T_f|=1$  are isovector. Endt adopted an empirical recommended upper limit (RUL) for each type of transition in a given mass region. He defined the RUL's such that the probability of the logarithmic reduced transition strengths exceeding the RUL was 0.001. It is conventional to express the transition strength in Weisskopf

TABLE II. Measured mixing ratios for primary  $\gamma$  rays. Those values marked with an asterisk (\*) rely on an assignment of  $J^\pi$  for the initial state either from shell-model calculations or from comparison with analog states. All other values are uniquely determined by experiment.

$E_i$ (keV)	$E_f$ (keV)	$\delta_\gamma$	$E_f$ (keV)	$\delta_\gamma$
6520.8	0	$0.05^{+0.05}_{-0.06}$	1454.2	$-0.08 \pm 0.09$
	2539.0	$-5^{+1}_{-3}$	2839.3	$8^{+6}_{-2}$
	2937.5	$0.10^{+0.06}_{-0.05}$	3835.8	$0.4^{+0.1}_{-0.2}$
	4182.8	$0.08 \pm 0.05$	4502.2	$-0.03 \pm 0.02$
6597.7	1973.3	$-0.45 \pm 0.05^*$	2839.3	$-0.3 \pm 0.1^*$
	3928.6	$-9^{+5}_{-\infty}$		
6667.8	2723.7	$30^{+\infty}_{-20}$	2937.5	$-0.04^{+0.02}_{-0.01}$
	3835.8	$-1.7^{+0.6}_{-1.5}$	4182.8	$0.00 \pm 0.02$
	5576.3	$0.0 \pm 0.1$		
6853.9	2723.7	$-1.8^{+0.9}_{-3.4}$	2937.5	$0.0 \pm 0.2$
	4502.2	$0.0 \pm 0.2$		
6873.4	2723.7	$-0.01^{+0.02}_{-0.03}$	2937.5	$0.05 \pm 0.02$
	5508.6	$-1.4^{+0.3}_{-0.4}$		
6978.3	5508.6	$6^{+4}_{-2}$		
7045.0	6093.5	$0.07^{+0.04}_{-0.03}$		
7203.0	2937.5	$0.06^{+0.04}_{-0.03}$		
7223.3	4143.6	$0.06 \pm 0.02$	4625.9	$0.00^{+0.02}_{-0.03}$
7282.0	2539.0	$0.23 \pm 0.08$	2723.7	$3.8^{+0.7}_{-0.6}$
	2839.3	$-1.4^{+0.3}_{-0.4}$	4182.8	$0.07^{+0.01}_{-0.02}$
	5576.3	$-0.18 \pm 0.09$		
7283.4	0	$-0.06 \pm 0.01$	708.7	$-0.01 \pm 0.07$
	1454.2	$-2.3^{+0.3}_{-0.5}$	2723.7	$-0.01 \pm 0.02$
	3835.8	$0.07 \pm 0.04$	4422.8	$0.05 \pm 0.01$
	4736.0	$-0.06 \pm 0.03$	4941.4	$0.4 \pm 0.1$
	5206.8	$-0.06 \pm 0.03$		
7493	2937.5	$-12^{+10}_{-\infty}$	4182.8	$6^{+\infty}_{-4}$
	4502.2	$2^{+21}_{-1}$		
7560.5	2937.5	$-0.06 \pm 0.04$	4182.8	$0.08^{+0.02}_{-0.01}$
	5508.6	$-2.0 \pm 0.3$	5576.3	$0.04^{+0.01}_{-0.02}$
	5934.0	$0.68^{+0.04}_{-0.05}$	6006.0	$-1.6 \pm 0.2$
7562.5	0	$-0.05 \pm 0.02$	1454.2	$-0.09 \pm 0.06$
	2937.5	$-360^{+350}_{-\infty}$	3019.2	$0.1 \pm 0.1$
	3835.8	$0.09^{+0.04}_{-0.03}$	3928.6	$-0.1^{+0.2}_{-0.1}$
	4422.8	$-1.3^{+0.5}_{-0.9}$	4736.0	$-0.03 \pm 0.03$
	5206.8	$-0.12 \pm 0.05$	5701.3	$-0.1 \pm 0.1$
7605.0	0	$-8 \pm 2$	2937.5	$-2.4 \pm 0.1$
	4182.8	$-2.1 \pm 0.2$	5508.6	$-0.02^{+0.04}_{-0.03}$
7636.0	3835.8	$0.04 \pm 0.03$	4182.8	$2.4^{+0.4}_{-0.3}$
	4422.8	$5^{+2}_{-1}$	4736.0	$0.17 \pm 0.05$
7644.2	2723.7	$0.00 \pm 0.02$	2839.3	$0.17 \pm 0.07$
	2937.5	$2.4^{+0.1}_{-0.2}$	3835.8	$0.07 \pm 0.02$
	4182.8	$7 \pm 1$	4422.8	$3.0 \pm 0.2$
7749.3	2723.7	$-1^{+1}_{-\infty}$	2937.5	$0.0 \pm 0.2$
	3019.2	$-1.0^{+0.5}_{-1.2}$	4502.2	$0.0 \pm 0.3$
7752.7	1973.3	$0.2 \pm 0.1$	5508.6	$1.2 \pm 0.3$
	5934.0	$-0.05 \pm 0.07$		
7759.0	1454.2	$0.00 \pm 0.02$	1973.3	$0.26 \pm 0.06$
	2539.0	$0.4 \pm 0.2$	2723.7	$0.01^{+0.02}_{-0.01}$
	2839.3	$-0.04 \pm 0.09$	3928.6	$0.2^{+0.2}_{-0.1}$
	4422.8	$0.07^{+0.09}_{-0.08}$		
7883.8	2539.0	$0.01 \pm 0.03$	2839.3	$-0.24^{+0.03}_{-0.02}$

TABLE II. (*Continued*).

$E_i$ (keV)	$E_f$ (keV)	$\delta_\gamma$	$E_f$ (keV)	$\delta_\gamma$
7920.9	4298.6	$-0.7^{+0.4}_{-0.5}$	4343.8	$-0.04^{+0.02}_{-0.03}$
	708.7	$0.13 \pm 0.08$	1973.3	$-1.2^{+0.5}_{-1.3}$
	2539.0	$0.00 \pm 0.08$	2937.5	$0.4 \pm 0.1$
7922	3835.8	$0.2^{+0.2}_{-0.1}$	4736.0	$8^{+60}_{-4}$
	2839.3	$0.11^{+0.04}_{-0.05}$		
7996.7	0	$0.2^{+0.1}_{-0.2}$	3019.2	$0.0 \pm 0.3$
8007.4	3733.8	$1.0^{+1.5}_{-0.6}$		
	0	$-20^{+10}_{-\infty}$	2937.5	$0.73 \pm 0.08$
	4182.8	$1.0 \pm 0.3$	5576.3	$1.6^{+1.1}_{-0.6}$
8014.3	5934.0	$-0.20 \pm 0.07$		
	0	$-0.30 \pm 0.06$	708.7	$1.4 \pm 0.2$
	4182.8	$-0.02 \pm 0.05$	5508.6	$-0.01 \pm 0.03$

units (W.u.) [39] since this factors out the mass and energy dependence of the various  $QL$  transition types. We converted our partial widths to Weisskopf units and applied the RUL technique. This eliminated a number of ambiguities in compound and final state  $J$  and  $\pi$  values. Since the RUL values are  $T$  dependent, this also eliminated possible  $T$  values in both initial and final states.

### C. Example

We illustrate the use of the RUL method with an example. The  $E_x=7282.0$  keV state had a previous assignment of  $J=3$ , with no information on  $\pi$  or  $T$  [26]. Six primary transitions were used in this analysis—all of the final states had known  $J$ ,  $\pi$ , and  $T$  values. The mixing ratio analysis was repeated twice, assuming  $3^+$  and  $3^-$  for the initial state. For the  $3^-$  assumption the  $\chi^2$  value was far above the 99%

confidence level for the appropriate number of degrees of freedom, while the  $\chi^2$  value for the  $3^+$  assumption was well below the 99% confidence limit. Therefore we adopted a  $3^+$  assignment.

The reduced transition strengths for the 7282.0-keV resonance are listed in Table IV. The RUL for an  $M1$ (IS) transition is 0.05 W.u., which is exceeded by the  $M1$  transition to the final state at 4182.8 keV. Since the final state has  $T=1$ , this suggests that the initial state must have  $T=0$ . With this information, one can also draw a conclusion about the transition to the 5576.3-keV final state. This state has  $T=1$  and the mixing ratio analysis gave two acceptable fits. However, if the initial state has  $T=0$ , then the transition must be isovector. The RUL for  $E2$ (IV) is 5 W.u., thus ruling out one of the mixing ratio solutions. Thus the angular distribution analysis for this resonance provided a parity and an isospin assignment, as well as the mixing ratios for five transitions.

TABLE III. Measured mixing ratios for secondary  $\gamma$  rays.

$E_i$ (keV)	$E_f$ (keV)	$\delta_\gamma$
708.7	0	$-1.0^{+0.8}_{-3.4}$
2723.7	0	$-4.8 \pm 0.4$
2839.3	1454.2	$-12^{+3}_{-6}$
2937.5	0	$0.3 \pm 0.2$
	708.7	$0.0^{+0.3}_{-0.2}$
3835.8	1454.2	$-4.1^{+0.9}_{-1.7}$
	708.7	$3.6^{+0.8}_{-0.5}$
	2937.5	$0.12 \pm 0.03$
4182.8	0	$0.1^{+0.1}_{-0.2}$
4422.8	708.7	$3.3^{+1.9}_{-0.9}$
	0	$10^{+2}_{-1}$
4502.2	0	$0^{+5}_{-4}$
	1454.2	$0.3^{+0.2}_{-0.1}$
4736.0	2937.5	$-0.02 \pm 0.03$
5508.6	1454.2	$0.06 \pm 0.05$
5576.3	708.7	$0.05 \pm 0.05$
5701.3	4182.8	$-1.3^{+0.8}_{-3.8}$
5934.0	1973.3	$2.0^{+0.9}_{-0.5}$

### V. ADOPTED QUANTUM NUMBER ASSIGNMENTS

The goal of the present experiment is the complete spectroscopy of the nuclide  $^{30}\text{P}$  from the ground state to 8.0 MeV. One must identify every state and obtain an assignment for the total angular momentum  $J$ , the parity  $\pi$ , and the

TABLE IV. Reduced transition strengths for the  $E_x=7282.0$  keV resonance. The angular distributions for the  $r \rightarrow 5577$  and  $r \rightarrow 1455$  transitions are each consistent with two values of  $\delta_\gamma$ ; both are listed here.

$E_f$ (keV)	$J^\pi; T$	$\delta_\gamma$	$B(M1)$ (W.u.)	$B(E2)$ (W.u.)
5576.3	$2^+; 1$	$+\infty$	0	37.4
		$-0.18 \pm 0.09$	0.023	1.2
4182.8	$2^+; 1$	$0.07^{+0.01}_{-0.02}$	0.082	0.17
2839.3	$3^+; 0$	$-1.4^{+0.3}_{-0.4}$	0.0023	1.0
2723.7	$2^+; 0$	$3.8^{+0.7}_{-0.6}$	0.00061	1.93
2539.0	$3^+; 0$	$0.23 \pm 0.08$	0.0083	0.089
1454.2	$2^+; 0$	$3.7 \pm 0.3$	0.0017	3.1
		$0.05 \pm 0.02$	0.02	0.01

TABLE V. Adopted assignments in  $^{30}\text{P}$ .

Compilation <sup>a</sup>		Experiment <sup>b</sup>			Shell model <sup>c</sup>		$^{30}\text{Si}$ <sup>d</sup>		Adopted assignments <sup>e</sup>	
$E_x$ (keV)	$J^\pi; T$	$E_x$ (keV)	$J^\pi; T$	Rat. <sup>f</sup>	$E_x$ (keV)	$J^\pi; T$	$E_x$ (keV)	$J^\pi; T$	$E_x$ (keV)	$J^\pi; T$
0	1 <sup>+</sup> ;0	0			0	1 <sup>+</sup> ;0			0	1 <sup>+</sup> ;0
677.29 (7)	0 <sup>+</sup> ;1	677.01 (3)			693	0 <sup>+</sup> ;1	677	0 <sup>+</sup> ;1	677.01 (3)	0 <sup>+</sup> ;1
709.02 (6)	1 <sup>+</sup> ;0	708.70 (3)			644	1 <sup>+</sup> ;0			708.70 (3)	1 <sup>+</sup> ;0
1454.67 (7)	2 <sup>+</sup> ;0	1454.23 (2)			1491	2 <sup>+</sup> ;0			1454.23 (2)	2 <sup>+</sup> ;0
1973.62 (11)	3 <sup>+</sup> ;0	1973.27 (4)			2061	3 <sup>+</sup> ;0			1973.27 (4)	3 <sup>+</sup> ;0
2539.03 (11)	3 <sup>+</sup> ;0	2538.95 (5)			2510	3 <sup>+</sup> ;0			2538.95 (5)	3 <sup>+</sup> ;0
2723.96 (10)	2 <sup>+</sup> ;0	2723.72 (7)			2461	2 <sup>+</sup> ;0			2723.72 (7)	2 <sup>+</sup> ;0
2839.9 (2)	3 <sup>+</sup> ;0	2839.34 (4)			2973	3 <sup>+</sup> ;0			2839.34 (4)	3 <sup>+</sup> ;0
2937.87 (6)	2 <sup>+</sup> ;1	2937.46 (2)			3003	2 <sup>+</sup> ;1	2912	2 <sup>+</sup> ;1	2937.46 (2)	2 <sup>+</sup> ;1
3019.39 (11)	1 <sup>+</sup> ;0	3019.2 (1)			3131	1 <sup>+</sup> ;0			3019.2 (1)	1 <sup>+</sup> ;0
3733.9 (3)	1 <sup>+</sup> ;0	3733.80 (7)			3737	1 <sup>+</sup> ;0			3733.80 (7)	1 <sup>+</sup> ;0
3835.9 (2)	2 <sup>+</sup> ;0	3835.80 (5)			4113	2 <sup>+</sup> ;0			3835.80 (5)	2 <sup>+</sup> ;0
3928.9 (3)	3 <sup>+</sup> ;0	3928.61 (5)			4285	3 <sup>+</sup> ;0			3928.61 (5)	3 <sup>+</sup> ;0
4143.67 (14)	2 <sup>-</sup> ;0	4143.63 (6)							4143.63 (6)	2 <sup>-</sup> ;0
4182.65 (8)	2 <sup>+</sup> ;1	4182.81 (6)			4243	2 <sup>+</sup> ;1	4176	2 <sup>+</sup> ;1	4182.81 (6)	2 <sup>+</sup> ;1
4232.2 (4)	4 <sup>-</sup> ;0	4231.97 (9)							4231.97 (9)	4 <sup>-</sup> ;0
4298.1 (10)	4 <sup>+</sup> ;0	4298.6 (2)			4593	4 <sup>+</sup> ;0			4298.6 (2)	4 <sup>+</sup> ;0
4343.6 (5)	5 <sup>+</sup> ;0	4343.8 (1)			4584	5 <sup>+</sup> ;0			4343.8 (1)	5 <sup>+</sup> ;0
4422.4 (3)	2 <sup>+</sup> ;0	4422.8 (1)			4358	2 <sup>+</sup> ;0			4422.8 (1)	2 <sup>+</sup> ;0
4468.33 (7)	0 <sup>+</sup> ;1	4469.1 (2)			4778	0 <sup>+</sup> ;1	4465	0 <sup>+</sup> ;1	4469.1 (2)	0 <sup>+</sup> ;1
4502.32 (12)	1 <sup>+</sup> ;1	4502.21 (9)			4903	1 <sup>+</sup> ;1	4447	1 <sup>+</sup> ;1	4502.21 (9)	1 <sup>+</sup> ;1
4626.55 (14)	3 <sup>-</sup> ;0	4625.92 (8)							4625.92 (8)	3 <sup>-</sup> ;0
4736.4 (2)	3 <sup>+</sup> ;0	4736.03 (8)			4862	3 <sup>+</sup> ;0			4736.03 (8)	3 <sup>+</sup> ;0
4926.4 (2)	5 <sup>-</sup> ;0	4925.5 (2)	3(5) <sup>-</sup> ;0	DE					4925.5 (2)	3 <sup>-</sup> ;0
		4937.3 (2)	(1,2 <sup>+</sup> ) <sup>g</sup>	CD					4937.3 (2)	1 <sup>-</sup> ;0 <sup>SA</sup>
4941.0 (3)	1 <sup>+</sup> ;0	4941.4 (3)	1 <sup>+</sup> ;0	CD	4931	1 <sup>+</sup> ;0			4941.4 (3)	1 <sup>+</sup> ;0
5028(3)	5(4,6) <sup>-</sup>								5028(3)	5 <sup>-</sup> ;0 <sup>A</sup>
5206.6 (4)	3 <sup>+</sup>	5206.8 (1)	3 <sup>+</sup> ;0	C					5206.8 (1)	3 <sup>+</sup> ;0
					5654	3 <sup>+</sup> ;1	5508	3 <sup>+</sup> ;1		
5231.6 (5)	4 <sup>-</sup>	5230.1 (3)	(2,4) <sup>-</sup> <sup>h</sup>	AC					5230.1 (3)	(2,4) <sup>-</sup> ;0 <sup>A</sup>
					5146	4 <sup>+</sup> ;0				
5411.1 (5)	0(2) <sup>-</sup>	5411.1 (3)	2 <sup>-</sup>	C					5411.1 (3)	2 <sup>-</sup> ;0 <sup>A</sup>
					5471	2 <sup>+</sup> ;0				
5506.1 (2)	1;0	5506.4 (2)	1 <sup>-</sup> ;0	A					5506.4 (2)	1 <sup>-</sup> ;0
5508.6 (4)	(2,3);1	5508.55 (8)	3 <sup>+</sup>	AC	5574	3 <sup>+</sup> ;0			5508.55 (8)	3 <sup>+</sup> ;0 <sup>M</sup>
5576 (2)	2 <sup>+</sup> ;1	5576.3 (1)	2 <sup>+</sup>	AC	5741	2 <sup>+</sup> ;1	5487	2 <sup>+</sup> ;1	5576.3 (1)	2 <sup>+</sup> ;1 <sup>SA</sup>
5595 (3)	4 <sup>+</sup>				5455	4 <sup>+</sup> ;0			5595 (3)	4 <sup>+</sup> ;0 <sup>S</sup>
5701.7 (4)	1 <sup>+</sup> ;0	5701.3 (2)	1 <sup>+</sup> ;0		5896	1 <sup>+</sup> ;0			5701.3 (2)	1 <sup>+</sup> ;0
5714 (3)	(5,7) <sup>+</sup>				5104	5 <sup>+</sup> ;0			5714 (3)	5 <sup>+</sup> ;0 <sup>S</sup>
5808 (3)	(3,5) <sup>+</sup>				5571	5 <sup>+</sup> ;0			5808 (3)	5 <sup>+</sup> ;0 <sup>S</sup>
5890 (12)	(1,2,3) <sup>+</sup> ;1				5888	3 <sup>+</sup> ;1	5909	3 <sup>+</sup> ;1	5890 (12)	3 <sup>+</sup> ;1 <sup>SA</sup>
5907.7 (8)	2 <sup>-</sup>								5907.7 (17)	2 <sup>-</sup> ;0 <sup>A</sup>
5934.0 (5)		5934.0 (1)	3 <sup>+</sup> ;0	AC	6166	3 <sup>+</sup> ;0			5934.0 (1)	3 <sup>+</sup> ;0
5993 (4)	(0,1,2) <sup>-</sup>								5993 (4)	(0,1,2) <sup>-</sup>
5997.1 (8)	1 <sup>+</sup> ;0+1		1 <sup>+</sup> ;0	D	6085	1 <sup>+</sup> ;0			5997.1 (8)	1 <sup>+</sup> ;0
6006.0 (5)		6006.0 (1)	3 <sup>+</sup>	AC	6310	3 <sup>+</sup> ;0			6006.0 (1)	3 <sup>+</sup> ;0 <sup>M</sup>
6050 (10)	(0,1) <sup>+</sup> ;1				6218	0 <sup>+</sup> ;1	6049	0 <sup>+</sup> ;1	6050 (10)	0 <sup>+</sup> ;1 <sup>SA</sup>
6051 (5)	(3,4,5) <sup>+</sup> (;1)				6199	4 <sup>+</sup> ;1	5957	4 <sup>+</sup> ;1	6051 (5)	4 <sup>+</sup> ;1 <sup>SA</sup>
					6221	4 <sup>+</sup> ;0				
6094.6 (5)	3 <sup>-</sup> ;1	6093.5 (1)	3 <sup>-</sup> ;1				6165	3 <sup>-</sup> ;1	6093.5 (1)	3 <sup>-</sup> ;1
6181 (4)	(5,6,7) <sup>+</sup>				6377	5 <sup>+</sup> ;0			6181 (4)	5 <sup>+</sup> ;0 <sup>S</sup>
6229.0 (5)	(3,5) <sup>+</sup>	6229.0 (3)	(3,5) <sup>+</sup>		6377	5 <sup>+</sup> ;0			6229.0 (3)	5 <sup>+</sup> ;0 <sup>S</sup>

TABLE V. (Continued).

Compilation <sup>a</sup>		Experiment <sup>b</sup>		Rat. <sup>f</sup>	Shell model <sup>c</sup>		$^{30}\text{Si}$ <sup>d</sup>		Adopted assignments <sup>e</sup>	
$E_x$ (keV)	$J^\pi; T$	$E_x$ (keV)	$J^\pi; T$		$E_x$ (keV)	$J^\pi; T$	$E_x$ (keV)	$J^\pi; T$	$E_x$ (keV)	$J^\pi; T$
					6289	$0^+; 0$				
6269.6 (8)	$(1^+, 2); 1$	6268.7 (4)	$2^-; 1$	AD					6268.7 (4)	$2^-; 1$
6295 (5)	$> 5$								6295 (5)	$> 5$
6299.3 (6)	$3^+; 0$	6299.3 (2)	$3^+; 0$						6299.3 (2)	$3^+; 0$
6361 (9)	$(4, 5, 6)^-$								6361 (9)	$(4, 5, 6)^-; 0^A$
6468 (3)	$5^+, 6^-$								6468 (3)	$6^-; 0^{SA}$
6481.4 (6)	$1^+; 0$								6481.4 (16)	$1^+; 0$
6519.4 (6)	$(1, 2)^+$	6520.8 (5)	$2^+; 0$	BD	6652	$2^+; 0$			6520.8 (5)	$2^+; 0$
6597.7 (5)	$(3, 5)^+$	6597.7 (5)	$(3, 4^+, 5^+)$	BD	6607	$4^+; 1$	6627	$4^+; 1$	6597.7 (5)	$4^+; 1^{SA}$
					6643	$4^+; 0$				
6607(3) <sup>i</sup>	$(3, 5)^+$				6574	$5^+; 0$			6607 (3)	$5^+; 0^S$
6656 (5)	$; 1$				6898	$2^+; 1$	6291	$2^+; 1$	6656 (5)	$2^+; 1^{SA}$
6667.8 (5)	$2^-, 3^+$	6667.8 (5)	$3^+$	B	7066	$3^+; 0$			6667.8 (5)	$3^+; 0^S$
6791 (5)	$> 5$								6791 (5)	$> 5$
6853.9 (5)	$1^+; 0$	6853.9 (5)	$1^+; 0$		7085	$1^+; 0$			6853.9 (5)	$1^+; 0$
6873.4 (5)	$3^+$	6873.4 (5)	$3^+; 0$	D					6873.4 (5)	$3^+; 0$
6877 (1)	$2^-$	6877 (1)	$2^-$						6877 (1)	$2^-; 0^A$
6921 (1)	$1^-; 0$	6921 (1)	$1^-; 0$						6921 (1)	$1^-; 0$
6978.3 (5)	$(3, 4)^+$	6978.3 (5)	$(3, 4)^+; 0$		7012	$4^+; 0$			6978.3 (5)	$4^+; 0^S$
6981 (5) <sup>j</sup>	$(5, 6, 7)^+$				6945	$5^+; 0$			6981 (5)	$5^+; 0^S$
7014.9 (5)	$2^-; 0$	7014.9 (5)	$2^-; 0$						7014.9 (5)	$2^-; 0$
7045.0 (5)	$(2, 3, 4)^-; 0$	7045.0 (5)	$4^-; 0$	BD					7045.0 (5)	$4^-; 0$
7049.4 (5)	$4^-; 1$	7049.4 (5)	$4^-; 1$				7180	$4^-; 1$	7049.4 (5)	$4^-; 1$
7119.1 (5)	$(1^+, 2, 3)^+$	7119.1 (5)	$(1^+, 2, 3)^k$		7068	$2^+; 0$			7119.1 (5)	$2^+; 0^S$
					7145	$0^+; 0$				
7178 (3)	$1^-; 1$	7179 (3)	$1^-; 1$						7179 (3)	$1^-; 1$
7199.1 (5)	$7^+(5^+, 6^+)$				7120	$6^+; 0$			7199.1 (5)	$6^+; 0^S$
7203.0 (5)	$2^+; 0$	7203.0 (5)	$2^+; 0$						7203.0 (5)	$2^+; 0$
7207.5 (5)	$0^+; 1$	7207.5 (5)	$0^+; 1$		7457	$0^+; 1$	7319	$0^+; 1$	7207.5 (5)	$0^+; 1$
7223 (1)	$2^-; 1$	7223.3 (5)	$2^-; 1$				7318	$2^-; 1$	7223.3 (5)	$2^-; 1$
7282.0 (5)	$3^-; 0$	7282.0 (5)	$3^+; 0$	BD	7263	$3^+; 0$			7282.0 (5)	$3^+; 0$
7283.4 (5)	$2^+; 1$	7283.4 (5)	$2^+; 1$		7213	$2^+; 1$	7214	$2^+; 1$	7283.4 (5)	$2^+; 1$
7304.9 (5)	$2^-; 0$	7304.9 (5)	$2^-; 0$						7304.9 (5)	$2^-; 0$
7306.3 (5)	$2^-; 0$	7306.3 (5)	$2^-; 0$						7306.3 (5)	$2^-; 0$
7322 (3)	$1^-$	7322 (3)	$1^-$				7421	$1^-; 1$	7322 (3)	$1^-; 1^A$
7347 (5)	$(5, 6, 7)^+$								7347 (5)	$(6, 7)^+^{SA}$
7370 (5)			$5^+$	E			7678	$5^+; 1$	7370 (5)	$5^+; 1^A$
7383.4 (5)	$(1, 2, 3)^+$	7383.4 (5)	$(2^+, 3^-); 1$	BD					7383.4 (5)	$3^-; 1^S$
7493 (1)	$1^+; 0$	7493 (1)	$1^+; 1$	D					7493 (1)	$1^+; 1$
7560.5 (5)	$3^+; 0$	7560.5 (5)	$3^+$	BD	7444	$3^+; 0$			7560.5 (5)	$3^+; 0^M$
7562.5 (5)	$2^+; 1$	7562.5 (5)	$2^+; 1$						7562.5 (5)	$2^+; 1$
7579.9 (5)	$2^-; 0$	7579.9 (5)	$2^-; 0$						7579.9 (5)	$2^-; 0$
7605.0 (5)	$(1, 2)^+; 0$	7605.0 (5)	$2^+; 1$	BD	7660	$2^+; 1$	7592	$2^+; 1$	7605.0 (5)	$2^+; 1$
7636.0 (2)	$3; 1$	7636.0 (5)	$3^+; (0)$	BD					7636.0 (5)	$3^+; 0^A$
7644.3 (5)	$3^+; 1$	7644.3 (5)	$3^+; 0$	D					7644.3 (5)	$3^+; 0$
7647 (5)	$(4, 5, 6)^-; (1)$						7721	$5^-; 1$	7647 (5)	$5^-; 1^A$
7688.2 (5)	$5^+$	7688.2 (5)	$4^-; 0$	BD					7688.2 (5)	$4^-; 0$
7742 (3)	$1^-$	7742 (3)	$1^-$						7742 (3)	$1^-; 0^A$
7749.3 (5)	$1^+; 0$	7749.3 (5)	$1^+; 0$		7732	$1^+; 0$			7749.3 (5)	$1^+; 0$
7752.7 (5)	$(3, 4)^+$	7752.7 (5)	$3^+; (1)$	D			7542	$3^+; 1$	7752.7 (5)	$3^+; 1^A$
7759.0 (5)	$3^+; 1$	7759.0 (5)	$3^+; 1$		7895	$3^+; 1$	7756	$3^+; 1$	7759.0 (5)	$3^+; 1$

TABLE V. (*Continued*).

Compilation <sup>a</sup>		Experiment <sup>b</sup>			Shell model <sup>c</sup>		<sup>30</sup> Si <sup>d</sup>		Adopted assignments <sup>e</sup>	
$E_x$ (keV)	$J^\pi; T$	$E_x$ (keV)	$J^\pi; T$	Rat. <sup>f</sup>	$E_x$ (keV)	$J^\pi; T$	$E_x$ (keV)	$J^\pi; T$	$E_x$ (keV)	$J^\pi; T$
7786.4 (5)	(2,3,4) <sup>-</sup>	7786.4 (5)	2(4) <sup>-</sup>	B					7786.4 (5)	2 <sup>-</sup> ;0 <sup>A</sup>
7803 (3)	(2,3,4) <sup>-</sup>	7803 (3)	(2,3,4) <sup>-</sup>						7803 (3)	(2,3,4) <sup>-</sup>
7826.3 (5)	2 <sup>-</sup> ;0	7826.3 (5)	2 <sup>-</sup> ;0						7826.3 (5)	2 <sup>-</sup> ;0
7873.7 (5)	4 <sup>-</sup>	7873.7 (5)	4 <sup>-</sup>						7873.7 (5)	4 <sup>-</sup> ;0 <sup>A</sup>
					7877	6 <sup>+</sup> ;0				
7883.8 (5)	(3,4) <sup>+</sup>	7883.8 (5)	4 <sup>+</sup>	BD	7691	4 <sup>+</sup> ;1	7900	4 <sup>+</sup> ;1	7883.8 (5)	4 <sup>+</sup> ;1 <sup>SA</sup>
7892 (3)	2 <sup>-</sup>	7892 (3)	2 <sup>-</sup>				8185	2 <sup>-</sup> ;1	7892 (3)	2 <sup>-</sup> ;1 <sup>A</sup>
7920.9 (5)	2 <sup>+</sup>	7920.9 (5)	2 <sup>+</sup> ;0	D	7701	2 <sup>+</sup> ;0			7920.9 (5)	2 <sup>+</sup> ;0
7921.8 (5)	3 <sup>+</sup> ;0	7921.8 (5)	3 <sup>+</sup> ;0		8027	3 <sup>+</sup> ;0			7921.8 (5)	3 <sup>+</sup> ;0
7922(1)	(3,4) <sup>+</sup>	7922 (1)	4 <sup>(+)</sup>	BD	7765	4 <sup>+</sup> ;0			7922 (1)	4 <sup>+</sup> ;0
7931 (3)	0 <sup>+</sup>	7932 (3)	0 <sup>+</sup>				8117	0 <sup>+</sup> ;1	7932 (3)	0 <sup>+</sup> ;1 <sup>A</sup>
7996.7 (5)	0 <sup>+</sup> ;1	7996.7 (5)	1 <sup>+</sup> ;1	DE	8302	1 <sup>+</sup> ;1	8311	1 <sup>+</sup> ;1	7996.7 (5)	1 <sup>+</sup> ;1
8001 (1)	1 <sup>-</sup> ;0	8001 (1)	1 <sup>-</sup>	D					8001 (1)	1 <sup>-</sup> ;0 <sup>A</sup>
8007.4 (5)	(1,2) <sup>+</sup> ;0	8007.4 (5)	2 <sup>+</sup> ;1	BD	8000	2 <sup>+</sup> ;1	7933	2 <sup>+</sup> ;1	8007.4 (5)	2 <sup>+</sup> ;1
8014.3 (5)	2 <sup>+</sup> ;0	8014.3 (5)	2 <sup>+</sup>	D	8134	2 <sup>+</sup> ;1	8300	2 <sup>+</sup> ;1	8014.3 (5)	2 <sup>+</sup> ;1 <sup>M</sup>

<sup>a</sup>Data are taken from Ref. [20] unless noted otherwise. In the listing in the compilation, the convention is that states below 5 MeV have  $T=0$  unless stated otherwise [40].

<sup>b</sup>These energies and  $J^\pi; T$  assignments represent the overall results of the various TUNL studies of the  $p+^{29}\text{Si}$  system (Refs. [21,22,25,26,41] and this work) combined with previous experimental work. No values are listed for  $E_x$  or  $J^\pi; T$  if we did not observe the level; no values are listed for  $J^\pi; T$  for states below 4.8 MeV as we did not independently test those assignments.

<sup>c</sup>Results are from Ref. [27].

<sup>d</sup>Energies in <sup>30</sup>Si are taken from Ref. [20] and are shifted up by 677 keV to align the ground state in <sup>30</sup>Si with the first  $T=1$  state in <sup>30</sup>P.

<sup>e</sup> $J^\pi; T$  assignments which depend on comparison with shell-model calculations for <sup>30</sup>P are marked with a superscripted *S*; those which depend on comparison with the <sup>30</sup>Si level scheme are marked with a superscripted *A*. The  $T$  assignments for several states are uniquely determined once  $T$  is assigned for the  $E_x=5576$  keV state; those assignments are marked with a superscripted *M*.

<sup>f</sup>Rationale: We use a series of codes to indicate which of the  $p+^{29}\text{Si}$  measurements were critical in further restricting the  $J^\pi; T$  values listed in the most recent compilation. No code is listed when we agreed with the previous assignment: A, angular distributions of feeding transitions; B, angular distributions of decay transitions; C, RUL analysis of feeding transitions; D, RUL analysis of decay transitions; and E, other arguments.

<sup>g</sup>The  $E_x=4937.3$  keV state must be  $T=1$  if  $J^\pi=1^+$  or if  $J^\pi=2^+$ . This state was listed in earlier compilations of <sup>30</sup>P at  $E_x=4937.9(3)$  keV but was removed in the most recent listing. We find definite evidence of its existence.

<sup>h</sup>The  $E_x=5230.1$  keV state must be  $T=0$  if  $J^\pi=2^-$ .

<sup>i</sup>This state is not listed in the most recent compilation because it has been identified as corresponding to our 6597.7 keV state. It appears to us, however, that it is not the same state, and so it is included here.

<sup>j</sup>This state is not listed in the most recent compilation. However, it does not appear to coincide with our 6978.3 keV state and so is included here.

<sup>k</sup>The  $E_x=7119.1$  keV state has  $T=0$  if  $J^\pi=1^+$ .

isospin  $T$  for each state. We also wish to consider the properties of the transition strengths. In order to perform the statistical analysis properly, the individual  $QL$  matrix elements are required, which means that the multipole mixing ratios are needed for as many transitions as possible.

A summary of the quantum number assignments is provided in Table V, which lists the previous status (Ref. [20]), assignments based on our measurements, predictions of the nuclear shell model, and comparison with the level scheme of the parent nuclide <sup>30</sup>Si. Below about 4.5 MeV our results are consistent with the unambiguous quantum number assignments provided by Endt. Therefore in the column labeled ‘‘Experiment’’ we simply list our new value for the energy without comment. In an attempt to provide some information concerning the origin of our  $J$ ,  $\pi$ , or  $T$  assignments, we use a simple code that indicates whether the assignment was based

on angular distributions or transition strengths and on feeding or decay transitions.

These assignments result from the combination of measurements that we have performed. There are additional arguments that are valuable and that should be reliable. Each  $T=1$  state must have a corresponding state of the same spin and parity in the parent nucleus <sup>30</sup>Si. The parent nuclide is rather well known. The primary use of this comparison was for the isospin assignment of states with a known spin and parity. We also had the results of a shell-model calculation [27]. In <sup>26</sup>Al extensive shell-model calculations agree very well [42] with the experimental energy levels and quantum numbers. We therefore anticipated that the positive parity states in <sup>30</sup>P would also agree well with the shell-model spectrum. In practice, this is the case. For a number of states where the spin had been limited but not definitively deter-

mined, we adopted the shell-model assignment. In a few cases where the parity was in question, we used the absence of a predicted positive parity state to make a negative parity assignment. A detailed discussion of the justification for the quantum number assignments for each level is given by Grossmann [43].

In the end we had an assignment for all but a few states. For three of these states, the spin assignments are for  $J > 5$ ; we can exclude these states without affecting statistical analyses. Four other states have negative parity and a range of possible  $J$  values; negative parity precludes any comparison with this set of shell-model calculations. Therefore we have  $J$ ,  $\pi$ , and  $T$  assignments for 103 states, with only four states with  $J \leq 5$  with unknown assignments. Statistical analyses of the eigenvalues and of the electromagnetic transitions will be performed in a subsequent paper.

## VI. SUMMARY

The  $^{29}\text{Si}(p, \gamma)^{30}\text{P}$  reaction was studied for 32 resonances in the energy range  $E_p = 1.0\text{--}2.5$  MeV. Angular distributions were measured for 156 primary and 74 secondary transitions. These angular distributions were analyzed in order to determine  $J^\pi$  assignments for initial and final states as well as the multipole mixing ratios of the mixed  $M1$ - $E2$  transitions. The resulting partial  $\gamma$ -ray widths (as well the partial widths of pure multipole transitions) were compared with recom-

mended upper limits (RUL's) on the  $\gamma$ -ray strengths. Results from this analysis were combined with our previous measurements of the  $^{29}\text{Si}(p, p_0)^{29}\text{Si}$  and  $^{29}\text{Si}(p, \gamma)^{30}\text{P}$  reactions in order to determine the spin  $J$ , parity  $\pi$ , and isospin  $T$  of each level. To eliminate remaining ambiguities, we then compared the  $^{30}\text{P}$  spectrum with the spectrum of states in the parent nucleus  $^{30}\text{Si}$ . We also compared the experimental  $^{30}\text{P}$  spectrum with the positive parity spectrum calculated with the shell model.  $J$ ,  $\pi$ , and  $T$  were assigned for 103 states up to an excitation energy of 8.0 MeV. The number of states with unassigned quantum numbers is very small (four states that may have spins in the angular momentum range under consideration). Therefore the present level scheme of  $^{30}\text{P}$  provides a second example of complete spectroscopy to complement the only other known case of  $^{26}\text{Al}$ .

## ACKNOWLEDGMENTS

We thank W. E. Ormand for providing the shell-model calculations, which were performed with the code OXBASH. We thank W. C. Beal, L. K. McLean, and C. R. Westerfeldt for help with the experiment. This work was supported in part by the U.S. Department of Energy, Office of High Energy and Nuclear Physics, under Grants No. DE-FG02-97-ER41033, DE-FG02-97-ER41042, and DE-FG02-96ER40990.

- 
- [1] E. P. Wigner, Oak Ridge National Laboratory Report No. ORNL-2309, 1957, p. 59; in *Statistical Theories of Spectra: Fluctuations*, edited by C. E. Porter (Academic, New York, 1965), p. 199.
- [2] T. A. Brody, J. Flores, J. B. French, P. A. Mello, A. Pandey, and S. S. M. Wong, *Rev. Mod. Phys.* **53**, 385 (1981).
- [3] T. Guhr, A. Müller-Groeling, and H. A. Weidenmüller, *Phys. Rep.* **299**, 189 (1998).
- [4] R. U. Haq, A. Pandey, and O. Bohigas, *Phys. Rev. Lett.* **48**, 1086 (1982).
- [5] O. Bohigas, R. U. Haq, and A. Pandey, *Phys. Rev. Lett.* **54**, 1645 (1985).
- [6] M. Lombardi, O. Bohigas, and T. H. Seligman, *Phys. Lett. B* **324**, 263 (1994).
- [7] O. Bohigas, M. J. Giannoni, and C. Schmit, *Phys. Rev. Lett.* **52**, 1 (1984).
- [8] P. M. Endt, P. de Wit, and C. Alderliesten, *Nucl. Phys.* **A459**, 61 (1986).
- [9] P. M. Endt, P. de Wit, and C. Alderliesten, *Nucl. Phys.* **A476**, 333 (1988).
- [10] G. E. Mitchell, E. G. Bilpuch, P. M. Endt, and J. F. Shriner, Jr., *Phys. Rev. Lett.* **61**, 1473 (1988).
- [11] J. F. Shriner, Jr., E. G. Bilpuch, P. M. Endt, and G. E. Mitchell, *Z. Phys. A* **335**, 393 (1990).
- [12] F. J. Dyson, *J. Math. Phys.* **3**, 1191 (1962).
- [13] A. Pandey, *Ann. Phys. (N.Y.)* **134**, 110 (1981).
- [14] T. Guhr and H. A. Weidenmüller, *Ann. Phys. (N.Y.)* **199**, 412 (1990).
- [15] C. Ellegaard, T. Guhr, K. Lindemann, J. Nygård, and M. Oxborrow, *Phys. Rev. Lett.* **77**, 4918 (1996).
- [16] H. Alt, C. I. Barbosa, H.-D. Gräf, T. Guhr, H. L. Harney, R. Hofferbert, H. Rehfeld, and A. Richter, *Phys. Rev. Lett.* **81**, 4847 (1998).
- [17] A. A. Adams, G. E. Mitchell, and J. F. Shriner, Jr., *Phys. Lett. B* **422**, 13 (1998).
- [18] C. I. Barbosa, T. Guhr, and H. L. Harney, *Phys. Rev. E* (to be published).
- [19] M. S. Hussein and M. P. Pato, *Phys. Rev. Lett.* **84**, 3783 (2000).
- [20] P. M. Endt, *Nucl. Phys.* **A633**, 1 (1998), and references therein.
- [21] R. O. Nelson, E. G. Bilpuch, C. R. Westerfeldt, and G. E. Mitchell, *Phys. Rev. C* **27**, 930 (1983).
- [22] S. C. Frankle, G. E. Mitchell, J. F. Shriner, Jr., E. G. Bilpuch, and C. R. Westerfeldt, *Phys. Rev. C* **45**, 2746 (1992).
- [23] J. P. L. Reinecke, F. B. Waanders, P. Oberholzer, P. J. C. Janse van Rensburg, J. A. Cilliers, J. J. A. Smit, M. A. Meyer, and P. M. Endt, *Nucl. Phys.* **A435**, 333 (1985).
- [24] J. A. Cameron, *Phys. Rev. C* **47**, 1498 (1993).
- [25] P. M. Wallace, E. G. Bilpuch, C. R. Bybee, G. E. Mitchell, E. F. Moore, J. D. Shriner, J. F. Shriner, Jr., G. A. Vavrina, and C. R. Westerfeldt, *Phys. Rev. C* **54**, 2916 (1996).
- [26] G. A. Vavrina, E. G. Bilpuch, C. R. Bybee, G. E. Mitchell, E. F. Moore, J. D. Shriner, J. F. Shriner, Jr., P. M. Wallace, and C. R. Westerfeldt, *Phys. Rev. C* **55**, 1119 (1997).
- [27] W. E. Ormand (private communication).

- [28] A. J. Ferguson, *Angular Correlation Methods in Gamma-Ray Spectroscopy* (North-Holland, Amsterdam, 1965).
- [29] R. Huby, Proc. Phys. Soc., London, Sect. A **67**, 1103 (1954).
- [30] J. M. Blatt and L. C. Biedenharn, Rev. Mod. Phys. **24**, 258 (1952).
- [31] L. C. Biedenharn, in *Nuclear Spectroscopy, Part B*, edited by F. Ajzenberg-Selove (Academic, New York, 1960), p. 732.
- [32] L. J. B. Goldfarb and R. C. Johnson, Nucl. Phys. **18**, 353 (1960).
- [33] W. R. Nelson, H. Hirayama, and D. W. O. Rogers, Stanford Linear Accelerator Center Report No. 265, 1985.
- [34] H. J. Rose and D. M. Brink, Rev. Mod. Phys. **39**, 306 (1967).
- [35] C. R. Westerfeldt, J. F. Shriner, Jr., and G. A. Vavrina, TUNL report, 1995 (unpublished).
- [36] J. F. Shriner, Jr., E. G. Bilpuch, C. R. Bybee, G. E. Mitchell, E. F. Moore, J. D. Shriner, and C. R. Westerfeldt, Nucl. Instrum. Methods Phys. Res. B **99**, 641 (1995).
- [37] C. R. Westerfeldt, R. O. Nelson, E. G. Bilpuch, and G. E. Mitchell, Nucl. Instrum. Methods Phys. Res. A **270**, 467 (1988).
- [38] P. M. Endt, At. Data Nucl. Data Tables **55**, 171 (1993).
- [39] V. F. Weisskopf, Phys. Rev. **83**, 1073 (1951).
- [40] P. M. Endt (private communication).
- [41] S. C. Frankle, Ph.D. thesis, North Carolina State University, 1991.
- [42] P. M. Endt, P. de Wit, and C. Alderliesten, Nucl. Phys. **A487**, 221 (1988).
- [43] C. A. Grossmann, Ph.D. thesis, North Carolina State University, 1999.